Proceedings of the 7th JFPS International
Symposium on Fluid Power, TOYAMA 2008
September 15-18, 2008

OS10-3

# DESIGN AND NANOMETER POSITIONING OF A LOW FRICTION PNEUMATIC CYLINDER EMBEDDED WITH AEROSTATIC BEARINGS

Ming-Chang Shih and Kei-Ren Pai

Department of Mechanical Engineering,
National Cheng-Kung University,
No.1, Ta-Hsueh Road, Tainan 701, Taiwan (R.O.C.)
(E-mail:mcshih@mail.ncku.edu.tw)

**ABSTRACT**

In the paper, a low friction pneumatic cylinder and a sliding table, and both of them are embedded with aerostatic bearings are designed. A low friction pneumatic table is constructed by combining the pneumatic cylinder and the sliding table. The characteristics for the friction force versus velocity of the pneumatic cylinder and the pneumatic table are measured. Moreover, a hybrid self-tuning fuzzy sliding mode controller with dead zone and load compensation is designed to precisely control the position of the pneumatic table. The experimental results have shown that the pneumatic table has positioning accuracy of 20 nm, the resolution of the pulse scale.

**KEY WORDS**

Nanometer Positioning, Pneumatic Table, Aerostatic Bearing

## INTRODUCTION

The development of the modern industry such as the semiconductor, communication and bio- medicine technology leads to the extensive study on the ultra-precision measurement and positioning technology of nanometer classes. Low friction elements and suitable control strategies are needed to be designed and developed to lower the friction force and thus to obtain better positioning accuracy. Compared to the hydraulic and electric driving system, the pneumatic driving system has the following advantages: low cost, clean, and easy in power transfer; therefore it can be applied in many industries. However, because of the compressibility and leakage of the air, the friction force, and the load disturbance, the pneumatic system is time variant and highly nonlinear [1-2]. Moreover, the difficulty of the cylinder position control is mainly caused by the friction force between the cylinder and the piston as well as the stick slip effect phenomenon during the motion control of the pneumatic cylinder[3-4]. Recently, various nonlinearity compensation strategies such as dithering compensation and friction force compensation have been analyzed and designed according to the nonlinear characteristics of pneumatic components to overcome the nonlinear effects and thus to get a higher positioning accuracy. In the articles [5-7], the effective friction compensation methods are introduced and combined with the designed control approaches. Besides, the low friction force actuator is developed to reduce the system friction force. The friction force can be further reduced through the installation of the aerostatic bearings in the pneumatic cylinder. Because there are thus no seals in this

pneumatic actuator, the actuator becomes a low friction actuator. The compressed air flows to the small gap between the bearing and the sliding guide, and the cylinder can thus float around the air film and on the guide surface of the table. Due to the air film between the bearing and the sliding guide, the relative motion is almost free of friction. Moreover, because the air is used as the medium, it can be applied at very high or very low temperature environment. In the paper, the pneumatic cylinder and the sliding table embedded with aerostatic bearing are designed. Besides, a hybrid nonlinear self-tuning fuzzy sliding mode controller with deadzone and load compensation is designed for the system. The experimental results show that the nanometer accuracy control is successfully completed.

.

## DESIGN OF A PNEUMATIC CYLINDER EMBEDDED WITH AEROSTATIC BEARINGS AND FRICTION MEASUREMENT ILLUSTRATIONS

The scheme of the designed pneumatic cylinder embedded with aerostatic bearings is shown in Figure 1. The air gap is found between the cylinder block and the piston, as well as between the piston rod and the right- and left- end covers of the cylinder. If the compressed air is supplied, the pneumatic piston rod and the piston tend to float in the air. The friction force becomes very small because there is not any contact between the cylinder and the piston rod.

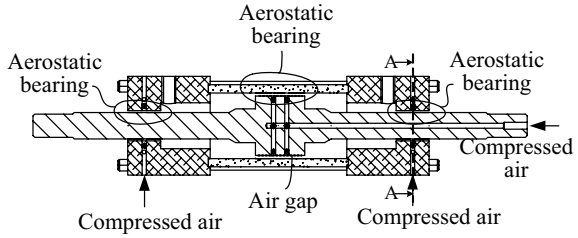


Figure 1 Scheme of the pneumatic cylinder embedded with aerostatic bearings.

Figure 2 shows the scheme of the measurement for the friction force of the pneumatic cylinder embedded with the aerostatic bearing. The compressed air flows through the pipes and the servo valve, and then flows into the pneumatic cylinder to drive the table, which is supported and guided by eight pieces of round aerostatic bearing pads. Moreover, a hydraulic cylinder is connected to this pneumatic cylinder to stabilize the motion of the pneumatic cylinder. The pulse scale is used to measure the position and the velocity by differentiating the position signals. The load cell is connected to the two pneumatic cylinders to indicate the friction force of the cylinder during motion. Figure 3 shows the experimental results of the relationship of the friction force versus the moving velocity of the cylinder. The friction force is found to be a function of the compressed air pressure. One can see that the static friction force at pressure 2, 3 and 4 bar are found to be 0.5 N, 1.0 N and 1.2 N, respectively. Generally, the friction forces of the aerostatic bearing cylinders are very small, and the difference between the static and dynamic friction forces is also very small. In this figure, the differences between the static and dynamic friction forces are in the range between 0.3N and 0.5 N.

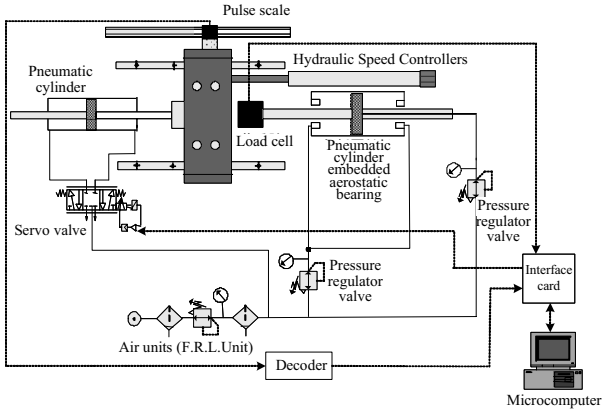


Figure 2 Scheme of friction force measurement.

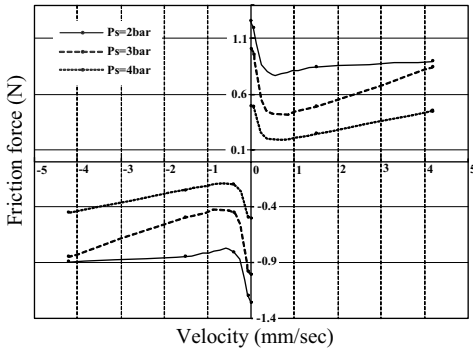


Figure 3 Friction force vs. velocity for a pneumatic cylinder with aerostatic bearing.

## CONSTRUCTION OF A LOW FRICTION PNEUMATIC SERVO TABLE EMBEDDED WITH AEROSTATIC BEARINGS PADS AND FRICTION MEASUREMENT

A low friction table driven by the pneumatic cylinder embedded with the aerostatic bearing is constructed. Figure 4(a) shows the structure of the table. Four pieces of round aerostatic bearing pads are installed to support the weight of the table in order that the table can be floated and moved along the guide of the base seat. Another 4 pieces of the round aerostatic bearing pads are installed at the two sides of the base seats to ensure the table sliding in the fitted direction. Figure 4(b) is the photograph of the constructed table.

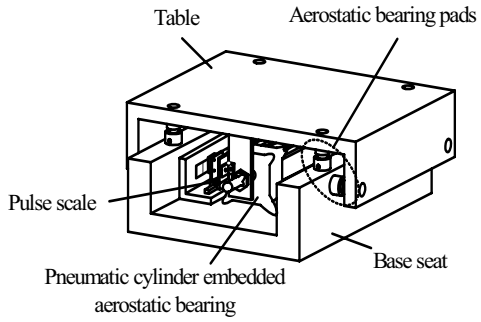


(a) Structure

(b) Photograph

Figure 4 Structure and photograph of the pneumatic table embedded with aerostatic bearings and pads.

Figure 5 shows the scheme of the friction force measurement of the table driven by the aerostatic bearing cylinder. The load cell is installed to measure the friction force. The pulse scale is used to measure the displacement and the velocity signal is obtained by the differentiation of the displacement. The pressure of the compressed air is 3 bar and the supply compressed air of the aerostatic bearing pad is 6 bar. The friction force versus the velocity is measured and shown in the Fig. 6. The maximum static friction force is about 3.144 N and the smallest dynamic friction force is 2.019 N. When the velocity of the cylinder is larger than 1.4 mm/sec, it is found that the friction force keeps almost the same. The viscous friction force tends to be constant even when the velocity is further increased to be 5 mm/sec.

## PRECISE POSITION CONTROL OF THE PNEUMATIC TABLE EMBEDDED WITH AEROSTATIC BEARINGS

The scheme of the position control system of the low friction pneumatic driven servo table is shown in Figure 7. The actuator is the low friction pneumatic servo cylinder, and the table is guided by the round aerostatic bearings. The position is measured by a pulse scale with a resolution of 20 nm.

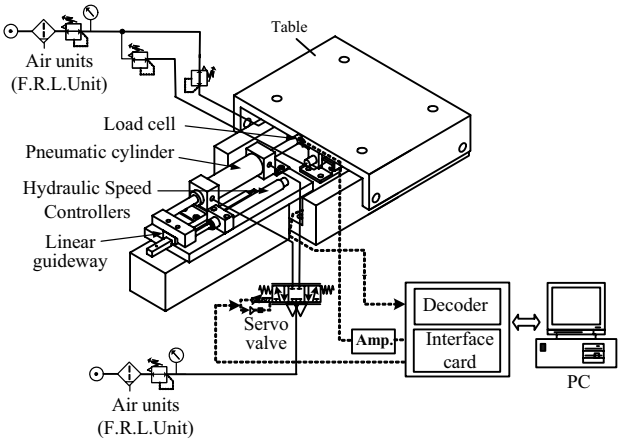


Figure 5 Scheme for measuring friction force vs. velocity of the table.

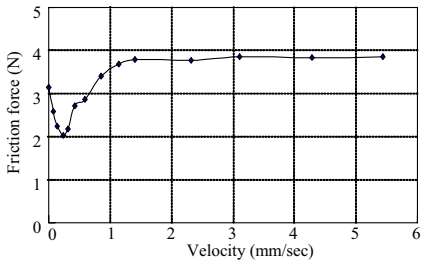


Figure 6 Friction force vs. velocity of the pneumatic cylinder driven table.

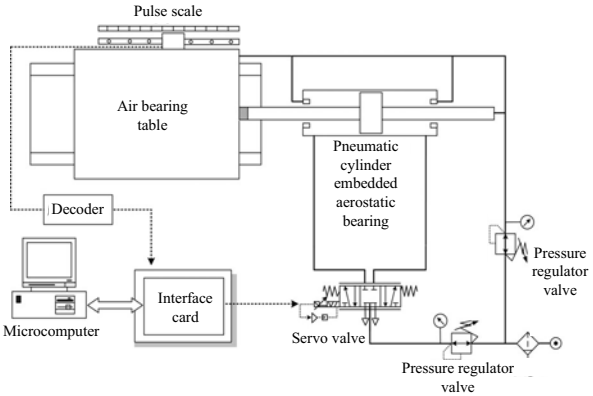


Figure 7 Scheme of the low friction pneumatic servo table.

Considering the nonlinear characteristic of the air flow through the servo valve and the compressibility of air, one knows that the system highly nonlinear and time variant. It is a great challenge for many researchers who have designed various nonlinear compensators to raise the accuracy of position control. In the paper, a self-tuning fuzzy sliding mode nonlinear controller compensated with the dead zone of valve and the variable load has been designed and implemented in the system to control the position of the table. The block diagram of the system is shown in Figure 8.

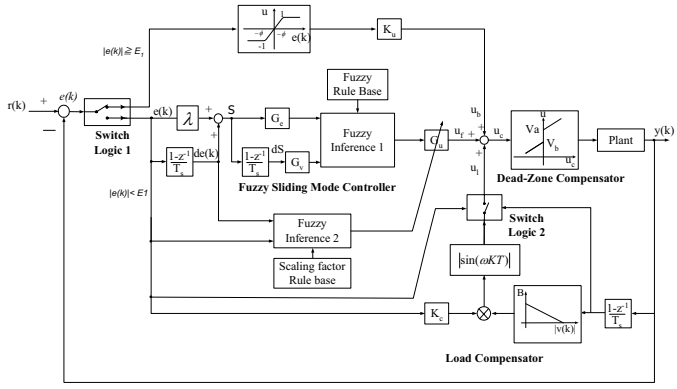


Figure 8 Block diagram of the pneumatic servo control system.

In the paper, a hybrid controller consisting of a hyperbolic tangent function and a self-tuning fuzzy sliding mode controller is designed to control the pneumatic table. One of them acts as a 'coarse' controller while the other acts as a 'fine' controller. A switching logic is applied to shift the control algorithm according to the error variable. The variable $E_1$ represents the boundary values of two mode control and *e(k)* is the position error. The choice of the value $E_1$ is according to the requirement of the rise time and the limit of overshooting. If $|e(k)| \geq E_1$, the positioning system performs speedily with its control signal designed by hyperbolic tangent algorithm at the start of control process. The positioning process tends to be decelerated near the boundary point. The algorithm of control signal in this stage is given by:

$$u_b = f(e(k)) = k_u \times \tanh\left(\frac{e(k)}{\phi}\right), \qquad (1)$$

where $k_u$ is the proportional gain and ø is the value of boundary layer. The proportional gain $k_u$ is set to decide the response speed of the system at the start of control process. Increasing $k_u$, the transient response can be accelerated but the undesired overshoot will also happen. Because of the above reason, the value of boundary layer *ø* is designed to execute the deceleration task for the control system when the system is near the boundary point *E1* so that the control system can smoothly go into the region of fine tuning and can avoid the appearance of overshoot.

As $|e(k)| < E1$, the switching logic is to shift the control algorithm and the self-tuning fuzzy sliding mode controller (SFSMC) is designed to execute the fine positioning control. The designed controller (SFSMC) includes the algorithm of the time variant gain factor ($\alpha(k)$) and the tuning of the scaling factors.

The fuzzy control theory was combined with the sliding mode control theory in the study to control the servo pneumatic system. The structure of the fuzzy control includes four parts: fuzzification inference, knowledge base, decision logic and defuzzification. In the article, Mamdani control rules and maximum-minimum algorithm are applied, and the "center of the gravity" method is used to defuzzify and to get the accurate control signal. For sliding mode control, the sliding surface *S* and the change of sliding surface *dS* are defined as

$$S(k) = de(k) + \lambda \times e(k), \qquad (2)$$

$$dS(k) = S(k) - S(k-1), \qquad (3)$$

where e(k) is the error, de(k) is the change of error and $\lambda$ is the slop of sliding surface S. The variables $S'(k)$, $dS'(k)$ and $U(k)$ are chosen to be the two inputs and one output of the fuzzy controller, respectively. The variables $S'(k)$ and $dS'(k)$ are defined by

$$S'(k) = S(k) \times Ge, \qquad (4)$$

$$dS'(k) = dS(k) \times Gv, \qquad (5)$$

where $Ge$ and $Gv$ are the scaling factors of sliding surface and the change of sliding surface. The control output signal $u_f(k)$ is defined as:

$$u_f(k) = U(k) \times Gu(k), \qquad (6)$$

where $U(k)$ and $Gu(k)$ denote the controller output and the output scaling factor of the controller at time instant *kT*. In this paper, the triangular membership function is applied to define the fuzzy sets of the inputs and the output, Figure 9 illustrated. Three linguistic fuzzy sets are applied for the input and output variables. The control rules are illustrated in Table 1. The "max-min" and "center of gravity" methods are adopted for fuzzy inference logic and defuzzification algorithm.

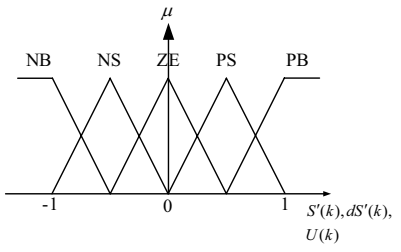


Figure 9 Membership function of $S'(k)$, $dS'(k)$ and $U(k)$.

Table 1 Fuzzy sliding mode control rules.

| S'(k) / U(k) / dS'(k) | NB | NS | ZE | PS | PB |
|---|---|---|---|---|---|
| NB | NB | NB | NS | NS | ZE |
| NS | NB | NS | NS | ZE | PS |
| ZE | NS | NS | ZE | PS | PS |
| PS | NS | ZE | PS | PS | PB |
| PB | ZE | PS | PS | PB | PB |

For the conventional fuzzy inference, its control parameters such as rules table, scaling factors and membership functions are usually obtained by trial-and-error method. The method is time- consuming and difficult to obtain the optimum parameters. Moreover, the conventional controller has not the adaptive resource to supervise and modify its control parameters to reject the disturbance. Therefore, in this paper the output scaling factor *Gu(k)* of fuzzy sliding mode controller is tuned on-line by a real-time gain updating factor *α(k)* to raise the positioning precision and robustness of the control system. The new scaling factors are modified by

$$Gu(k+1) = Gu(k) \times (1 + \alpha(k)), \tag{7}$$

where α(k) is the real-time gain factor. The value of real-time gain factor α(k) is computed on-line using a model independent fuzzy rule-base defined by error and change of error of the controlled variable. The most important point to note is that real-time gain factor is not dependent in any way on any process parameter. The value of real-time gain factor depends only on the input variable of controller at the sampling instant. The membership functions for input variables *e(k)* and *de(k)* and output variable *α(k)* are shown in Figure 10. The membership function for *α (k)* is also a triangular type and the rule-base in Table 2 is used for the computation of *α (k)*.

When a loading is applied on the pneumatic control system, the control characteristic will be varied due to the variation of operating pressure, and caused a obvious effect on the positioning precision. Therefore the load compensator, which is similar to the dither signal, is designed according to the error (*e(k)*) and the velocity (*V(k)*) to overcome the variation in this paper. The algorithm of load compensator is expressed by the following equations:

$$u_l = \begin{cases} e(k) \times K_c \times B(k) \times |\sin(\omega k T)|, & for\ |V(k)| \le V_1\ and\ |e(k)| \ge E_2 \\ 0, & for\ |V(k)| > V_1\ or\ |e(k)| < E_2 \end{cases}, \tag{8}$$

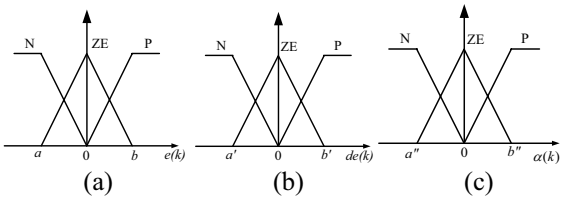


Figure 10 (a) Membership function of *e(k)*. (b) Membership function of *de(k)*. (c) Membership function of *α(k)*.

Table 2 Fuzzy rules of real-time gain factor.

| e(k) / de(k) / α(k) | N | ZE | P |
|---|---|---|---|
| N | ZE | N | ZE |
| ZE | P | ZE | P |
| P | ZE | N | ZE |

where $K_c$ is the gain of the amplitude and *B(k)* is the variable amplitude. The algorithm of the variable amplitude *B(k)* is expressed as:

$$B(k) = -\frac{\delta}{V_1} V(k) + \delta, \tag{9}$$

where $\delta$ is the maximum peak value of variable amplitude *B(k)*. When the loading effect causes the control system to lie at the stop state and the error is bigger than the desired steady state error($E_2$), the compensation signal is triggered and thus set to be the maximum value to ensure that the system never stops. As the control system is driven again from the stop state, the amplitude of load compensation signal is appropriately attenuated with the change of velocity to prevent the overshoot or oscillation phenomenon.
Finally, the deadzone compensation can be designed to avoid the deadzone. The algorithm of control voltage with deadzone compensation can be expressed by the following equation:

$$u = \begin{cases} u_c + V_a, & if\ u_c > 0 \\ u_c + V_b, & if\ u_c < 0 \end{cases}, \tag{10}$$

where $u_c$ is the output signal of controller and load compensator, and $V_a$ and $V_b$ are the compensation values of the dead zone at each side of the center.

## EXPERIMANTAL RESULTS OF NANOMETER POSITIONING

The above-described controller design is implemented in the microcomputer to control the position of the pneumatic servo table. The air supply pressure is set to

be 5 bar, the sampling time and the reference input are chosen to be 20 ms and 10 mm. The experimental results are shown in Figure 11. The position error is within the range of the resolution 20 nm of the pulse scale from the time instant 1.5 sec. In the fine feed experiment, the feed resolution is noticed through the various step feeds. From Figure 12 one can see that the low friction pneumatic servo table can be controlled to move step by step for 20 nm and the position error is about 20 nm.

Although the positioning accuracy less than 20nm is not possible in these positioning experiments owing to the restriction of the resolution of the pulse scale, it can be predicted that this positioning method has the ability of 20nm or even less feed resolution.

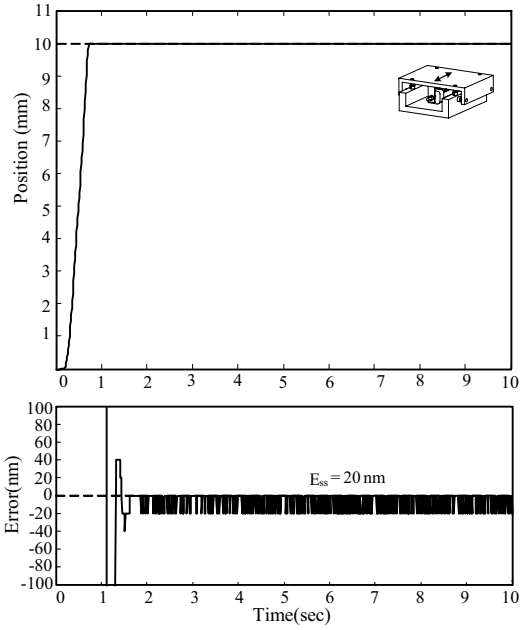


Figure 11 (a) Time response of the pneumatic servo table for a step input 10 mm. (b) Time response of error.

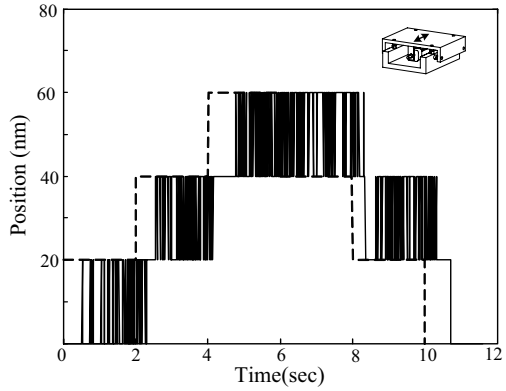


Figure 12 Multi-step responses of the pneumatic table with 20 nm step displacement.

## CONCLUSIONS

In the paper, we have fitted the pneumatic cylinder and the low friction driven table with aerostatic bearings, and have designed appropriate devices to measure their corresponding small friction forces. Moreover, this work has designed and implemented a hybrid self-tuning fuzzy sliding mode controller with the dead zone and load compensator for the precision control of the pneumatic table. The experimental results have shown that the pneumatic servo table can be controlled to the nanometer accuracy of 20 nm both with 10 mm step input and 20 nm stepwise input successfully.

## ACKNOWLEDGEMENT

This research was supported by National Science Council Taiwan, ROC, under the Grant NSC 94-2212-E-006-033.

## REFERENCES

1. Shearer J. J., “The Study of Pneumatic Process in the Continuous Control of Motion with Compressed Air-I”, ASME Trans., pp. 233-242 (1956).
2. Moore, P.R., PU, J. and Harrison, R.,”Progression of servo pneumatics forwards advanced applications”, in EDGE, K., and BURROWS, C. (Eds.): “Fluid power circuit, component and system design” (Research Studies Press,), ISBN 0863801390, pp.347-365 (1993).
3. Fujita T., Tokashiki R., and Kagawa T., ”Stick-slip Motion in Pneumatic Cylinders Driven by Meter-Out Circuit”, Proc. of the 4th JHPS International Symposium on Fluid Power, Tokyo, pp.131-136 (1999).
4. Kazama T, and Fujiwara M., “Experiment on Frictional Characteristics of Pneumatic Cylinders”, Proc. of the 4th JHPS International Symposium on Fluid Power, Tokyo, pp.453-458 (1999).
5. Ning S., and Bone G.M., ” High Steady-State Accuracy Pneumatic Servo Positioning System with PVA/PV Control and Friction Compensation”, Proceedings-IEEE International Conference on Robotics and Automation, Vol. 3, pp.2824-2829 (2002).
6. Xiang F., and Wikander J., ”Block-oriented approximate feedback linearization for control of pneumatic actuator system”, Control Engineering Practice, Vol.12, No. 4, pp.387-399 (2004).
7. Shih M.C., and Pai K.R., “Nanoaccuracy Position Control of A Pneumatic Cylinder Driven Table”, International Journal of JSME, Series C, Vol.46, No.3, p.1062-1068, (2003).